

# Design optimization of floating offshore wind farms using a steady state movement and flow model

**Feng, Ju; Pedersen, Mads Mølgaard; Riva, Riccardo; Bredmose, Henrik; Santos, Pedro**

*Published in:*
EERA DeepWind Conference 2024

*Link to article, DOI:*
10.1088/1742-6596/2875/1/012039

*Publication date:*
2024

*Document Version*
Publisher's PDF, also known as Version of record

**PAPER** • **OPEN ACCESS**

# Design optimization of floating offshore wind farms using a steady state movement and flow model

To cite this article: Ju Feng *et al* 2024 *J. Phys.: Conf. Ser.* **2875** 012039



Journal of Physics: Conference Series **2875** (2024) 012039 doi:10.1088/1742-6596/2875/1/012039

# Design optimization of floating offshore wind farms using a steady state movement and flow model

**Ju Feng**[1], **Mads Mølgaard Pedersen**[1], **Riccardo Riva**[1], **Henrik Bredmose**[1] **and Pedro Santos**[2]

[1] Department of Wind and Energy Systems, Technical University of Denmark, 2800 Kgs. Lyngby, Denmark

[2] DHI A/S, 2970 Hørsholm, Denmark

E-mail: jufen@dtu.dk (Ju Feng)

**Abstract.** In this study, we demonstrate how to carry out the design optimization of floating offshore wind farms by considering the impacts brought by the movements of the floating wind turbines. A steady state movement and flow model is applied in the modelling process. This model is developed by building a turbine surrogate model for estimating the steady state movement and power production of floating wind turbines and incorporating it in an open-source static wind farm simulator, `PyWake`. Using this modelling methodology, layout optimization problems of floating offshore wind farms are solved by using algorithms like Random Search to maximize the energy yield while satisfying certain constraints. Case studies are carried out for two wind farms with met-ocean conditions from a real planned site in Scottland to show the potential of layout optimization for floating wind farms.

## 1. Introduction

Floating wind has achieved a lot of progress in technical maturity and cost competitiveness, since Hywind Scotland, the world's first floating wind farm, was commissioned in 2017 [1]. Thus, we are now witnessing a great surge of interest in floating wind both in the industry and academia [2]. With many floating offshore wind farms (FOWFs) planned in the pipeline, we can undoubtedly expect that the research and development efforts in floating wind will expand from the current turbine centered viewpoints to farm level considerations.

To further decrease the levelized cost of energy (LCOE) and improve the reliability of floating wind, the overall design optimization of FOWFs constitutes an essential task. While the design optimization of bottom-fixed offshore wind farms has already been extensively studied [3], the same problem for FOWFs has received relatively few investigations. Among the limited literatures dealing with the design optimization of FOWFs, most of them either ignore the movements of the floater or only consider part of the movements [4]. However, as a unique feature for FOWFs, the floaters' movements, induced by the aerodynamic and hydrodynamic forces and constrained by the mooring systems, will introduce some non-negligible effects on the wake flow and power production for the FOWF. Thus, a proper design optimization of FOWFs needs to include the movement of floaters in the modelling chain and consider the mooring systems of each floating offshore wind turbine (FOWT) as part of the design variables.

In this study, we use a steady state movement and flow model [5] in the modelling of FOWFs. This model is developed by incorporating the movements of the floater in `PyWake` [6], an open-sourced

steady state wind farm simulation tool developed at DTU that can compute the flow field and power production of a given wind farm. The movements of the floater are obtained by an ANN (artificial neural network) based surrogate model trained using HAWC2 simulations [5]. The inputs of this surrogate model include: wind speed, wind direction, current speed and current-wind misalignment, while its outputs include: downwind, crosswind and upwards displacements of the rotor center, tilt and yaw angles of the rotor, and electrical power and aerodynamic thrust of the turbine.

The layout optimization problem of FOWFs to maximize AEP (annual energy production) while satisfying constraints on wind farm boundary and minimal spacing is formulated and solved with the Random Search algorithm [7]. The used FOWT is the IEA 15 MW reference wind turbine [8] with the WindCrete spar floater [9]. Case study at the Havbredey FOWF project site in Scotland [10] is carried out to demonstrate the effectiveness of the proposed methodology.

## 2. Modelling Methodology

Modelling the flow and power production of a FOWF requires properly considering impacts brought by the movements of the FOWTs. This section describes the modelling methodology used in this study.

### *2.1. Turbine model*

In this study, we select the widely used IEA 15 MW reference turbine [8] mounted on the WindCrete spar-buoy floater [9], as shown in Figure 1. Note that the floater has a total draft of 155 m and is equipped with 3 catenary mooring lines. The sea depth is assumed to be 200 m. Details on the WindCrete spar-buoy floater are referred to [9].

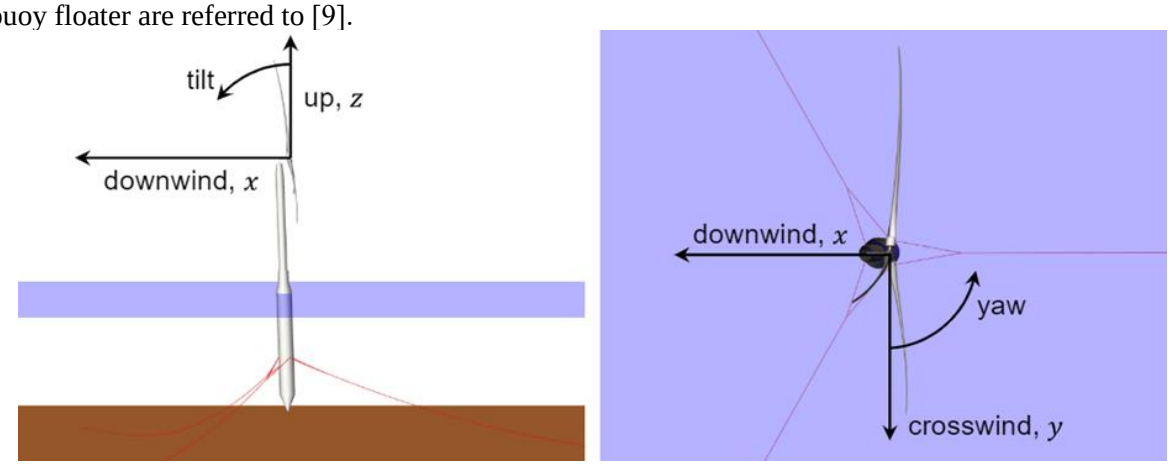


**Figure 1.** Selected floating offshore wind turbine (IEA 15 MW reference turbine with WindCrete spar-buoy floater) and the assumed coordinate frame [5].

The key parameters of the IEA 15 MW reference turbine are listed in Table 1, while its power curve and thrust curve are shown in Figure 2.

**Table 1.** Properties of the IEA 15 MW reference turbine

| Parameter | Value | Unit |
|---|---|---|
| Rated power | 15 | MW |
| Cut-in, rated, cut-out wind speeds | 3, 11, 25 | m/s |
| Rotor diameter | 240 | m |
| Hub height | 150 | m |

### *2.2. Steady state movement model*

Nowadays, the state-of-the-art aeroelastic codes such as HAWC2 [11] can dynamically simulate the motions and power production of a FOWT under a typical met-ocean condition (considering wind, wave and current) with reasonable accuracy. However, the associated computational cost makes it hard

to directly incorporate them in wind farm design optimization, as a single AEP computation of a wind farm requires evaluating multiple FOWTs under thousands of met-ocean conditions.

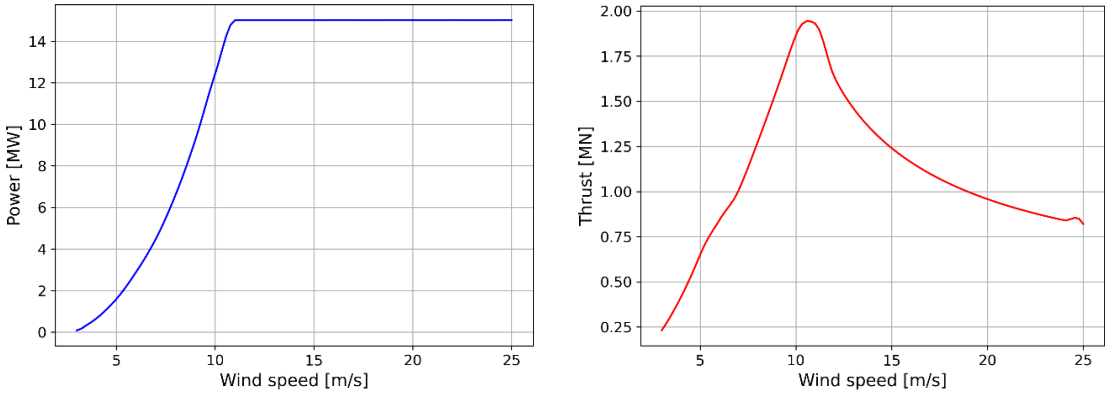


**Figure 2.** Power curve (left) and thrust curve (right) of the IEA 15 MW reference turbine.

To tackle this challenge, the surrogate-based method recently proposed by Riva et al. in [5] is used. This method simulates the steady state movement and flow of a FOWF with a static wind farm simulator, `PyWake` [6], and a turbine surrogate. The turbine surrogate is built for a given FOWT to predict its steady state displacements, rotations, thrust and power output under different met-ocean conditions. The procedure to build such a surrogate is described in Figure 3.


**Figure 3.** Procedure for building a turbine surrogate using ANN (Artificial Neural Network).

In this study, we use the surrogate built for the selected FOWT [5], i.e., IEA 15 MW reference turbine mounted on the WindCrete spar-buoy floater. This surrogate is built based on a database of `HAWC2` simulations, covering different ranges of met-ocean conditions as listed in Table 2. Nearly 60000 points from the input domain are sampled and the sampling strategy is referred to [5]. In these simulations, turbulence intensity and waves are set to zero and the vertical wind shear exponent is fixed at 0.1.

**Table 2.** Ranges of met-ocean conditions covered by the HAWC2 simulations

| Met-ocean condition | Value range | Unit |
|---|---|---|
| Wind speed | [3, 25] | m/s |
| Wind direction | [0, 360] | deg |
| Current speed | [0, 2] | m/s |
| Current-wind misalignment | [0, 360] | deg |

Using the obtained database, the turbine surrogate, i.e., a feed-forward neural network with fully-connected layers, is trained using `TensorFlow` [12]. A complete description of the simulation setup and the surrogate building process can be found in [5]. The turbine surrogate takes the following inputs: wind speed (experienced by the turbine rotor), wind direction, current speed and current-wind misalignment, and predicts the following outputs in steady state: downwind, crosswind, and upward displacements of the rotor center, the rotor tilt, yaw, power output, and thrust.

As an example, Figure 4 shows the steady state movements of the selected FOWT under different wind speeds and with or without a constant current. Note that in this example, the wind direction and current-wind misalignment angle are both assumed as 0 deg.

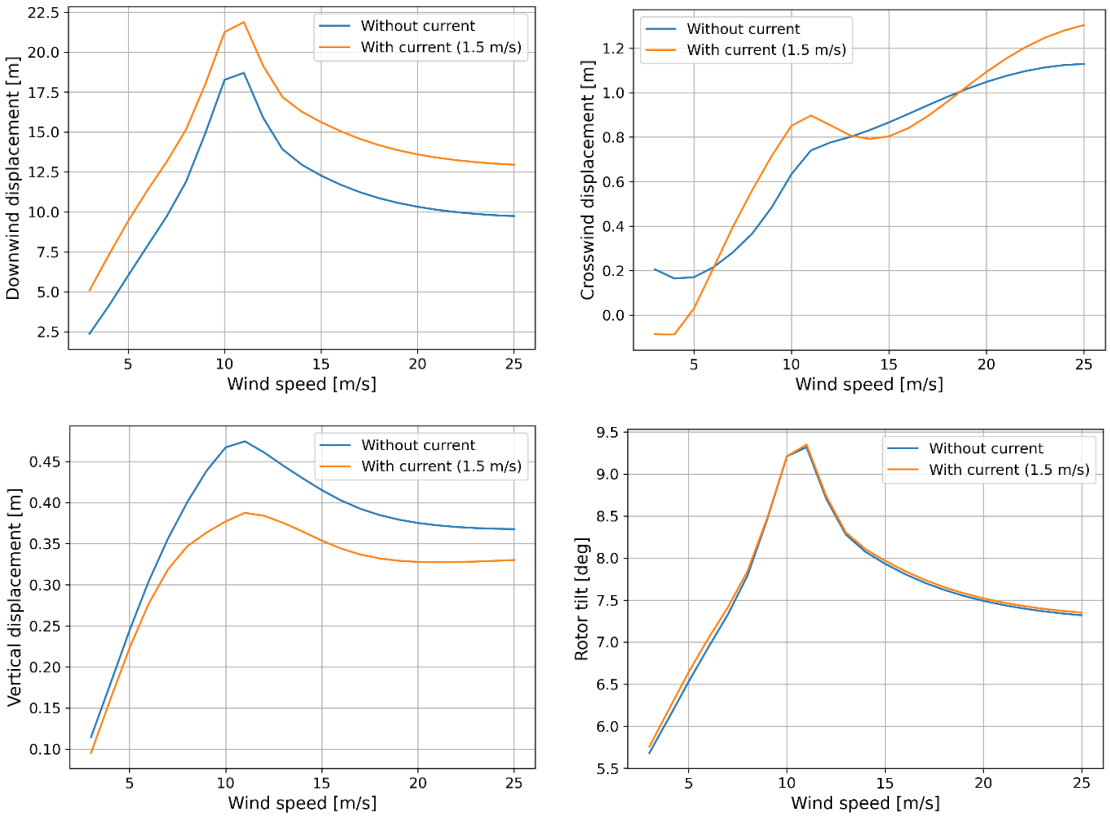


**Figure 4.** Steady state movements of the selected FOWT predicted by the turbine surrogate as functions of wind speed under perfectly aligned wind and current (wind direction at 0 deg).

*2.3. Flow modelling and AEP calculation*

Using the steady state movement model, i.e., the turbine surrogate built previously, we can then model the wind farm flow and calculate the AEP for a given FOWF. Following the method proposed in [5], 3 steps need to be carried out to simulate the steady state flow and power output of a FOWF under a given met-ocean condition:

- **Step 1**: build a turbine surrogate for the FOWT, which can predict the steady state displacements, rotations, thrust and power output under a given met-ocean condition the FOWT experiences;
- **Step 2**: couple the turbine surrogate model with `PyWake` to adjust the positions and orientations of each FOWT and simulate the resulted wake flows, which bend upwards due to tilted rotors, and power output of the FOWF;
- **Step 3**: iteratively solve for the steady state displacements and rotations using the coupled surrogate and `PyWake`, as the changes in position and orientation of a FOWT will change the inflow condition it experienced, as well as the wake behind it.

Essentially, the above steps constitute a steady state movement and flow model for FOWFs. Although the example in [5] is done for a specific type of FOWT, the same methodology is equally applicable to another type of FOWT, using other aeroelastic tools and/or other types of surrogate models.

As the steady state flow in the FOWF and the power outputs of all FOWTs can be computed using the previously described model, we can then calculate the AEP of the FOWF by considering the possible met-ocean conditions and their probability distribution. In this study, we limit our modelling to consider only different wind speeds and wind directions, while other met-ocean conditions, i.e., wind shear, current speed and current-wind misalignment, are assumed with fixed values.

To evaluate the computational cost of the model, AEP calculations for FOWFs composed of varying numbers of turbines are carried out. Two versions of simulations are done: the fixed version ignores the movements of FOWTs and treats them as bottom-fixed; the floating version considers the movements of FOWFs. Figure 5 shows the respective computational time as function of turbine number, with linear

(left) and logarithmic (right) scale both included. Note that the results are obtained by running the simulations on a laptop with an Intel® Core™ i5-1145G7 Processor with no parallelization.

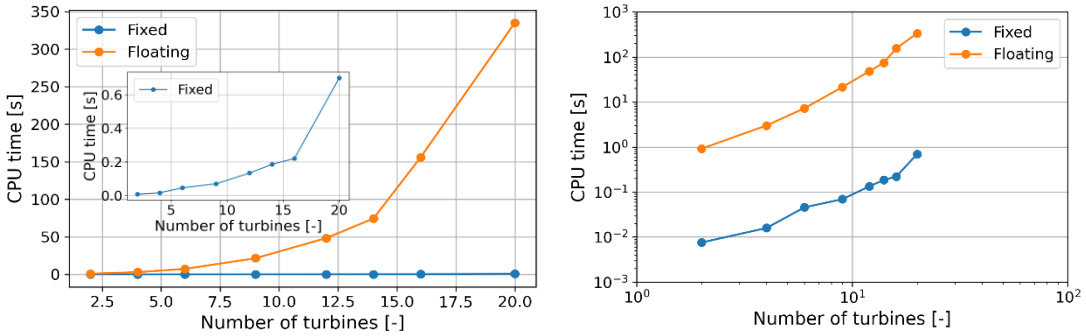


**Figure 5.** Speed of AEP calculation for FOWFs (treating FOWTs as bottom-fixed or floating).

As we can notice in Figure 5, the computational time of an AEP calculation for a FOWF increases polynomially with the number of turbines, likely because the wake effects between each two turbines need to be accounted. Also, considering the movements of FOWTs slows down the AEP calculation significantly, for example, the floating version calculation takes 355.3 seconds for a FOWF with 20 turbines, while its fixed version takes only 0.7 seconds. Nevertheless, we should note that the computational cost is still quite affordable for the floating version calculations and can be used in design optimization applications. Furthermore, parallelization will be able to further speed-up the computation.

## 3. Design optimization

### *3.1. Problem formulation*

Design optimization of a FOWF can include many different aspects, such as mooring lines for each turbine, anchor selections and positions, dynamical and static electrical cables, floating sub-station(s), and so on. In this study, we limit the scope to layout optimization, i.e., determining the optimal positions for each turbine. In the context of floating wind, the position of a FOWT means its nominal position, i.e., the position when it idles under no impacts of wind, wave or current.

Consider a FOWF composed of $N_{wt}$ FOWTs, its layout can be defined by the $x$ and $y$ coordinates of all turbines at their nominal positions and denoted as $\boldsymbol{L} = [\boldsymbol{X}, \boldsymbol{Y}] = [x_1, x_2, \dots, x_{N_{wt}}, y_1, y_2, \dots, y_{N_{wt}}]$. Then, a layout optimization problem to maximize AEP can be formulated as:

$$\max_{\boldsymbol{L}} \text{AEP}(\boldsymbol{L}) \tag{1}$$

A realistic wind farm layout optimization problem also needs to consider various constraints , which may be due to technical, environmental, regulatory and other considerations. In this study, we include two commonly considered constraints: wind farm boundary and minimal spacing requirements. Typically, a wind farm project is constrained to install all turbines inside a specified boundary, which is usually given by the energy planning authority. While the real wind farm boundaries can come at many different shapes, here we assume that the boundary is a circle, defined by a center $[x_{cen}, y_{cen}]$ and a radius $R_{bdr}$. Thus, this constraint is given as:

$$\sqrt{(x_i - x_{cen})^2 + (y_i - y_{cen})^2} \leq R_{bdr}, \quad \text{for } i = 1, 2, \dots, N_{wt} \tag{2}$$

We should also note that here the boundary is defined for the nominal positions of turbines. If the wind farm boundary should be applied to all anchors, we can simply adjust the value of radius $R_{bdr}$, by deducing the radius from a FOWT's floater center to its anchor positions.

Minimal spacing requirements ensure any two turbines inside a wind farm has a minimal spacing of $d_{min}$ between them, as governed by:

$$\sqrt{(x_i - x_j)^2 + (y_i - y_j)^2} \geq d_{min}, \quad \text{for } i, j = 1, 2, \ldots, N_{wt} \text{ and } i \neq j \tag{3}$$

*3.2. Optimization algorithm*

To solve the constrained layout optimization problem, we apply the Random Search (RS) algorithm, which was first proposed by Feng and Shen to solve constrained wind farm layout optimization problems [7]. It was extended later also to solve multi-objective layout optimization problems [13] and showed better performance than several other algorithms in a comparative study [14]. Figure 6 demonstrates the basic concept of this algorithm.

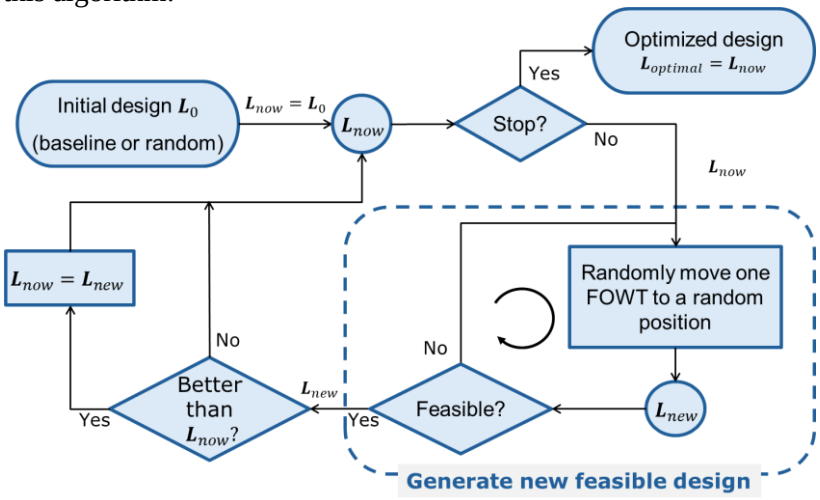


**Figure 6.** Flowchart of the Random Search (RS) algorithm for layout optimization of FOWFs.

## 4. Case study

*4.1. Site condition*

For case study, a Scottish site close to the planned Havbredey FOWF project is selected. DHI A/S has done a preliminary met-ocean study for this site [10]. The preliminary met-ocean study is consisted of utilising existing datasets to establish normal and extreme met-ocean conditions. In total, 20 years (2001-01-01 to 2021-12-31) of time series of hindcast data and analyses of normal and extreme conditions of wind, water levels, currents and waves were used in the met-ocean study [10].

For the purposes of this study, the joint distribution of wind speed and wind direction is derived using the provided time series of wind speed and wind direction. Since the mean wind speed at this site is quite high (13.58 m/s), well above the rated wind speed of the considered IEA 15 MW reference turbine, a reduced wind condition is also constructed by scaling down the corresponding wind speeds for the derived joint distribution, which results a wind condition with similar wind rose as the original one but a reduced mean wind speed (7.29 m/s). Figure 7 shows the joint distribution of these two scenarios.

Based on the preliminary met-ocean study of this site [10], the most representative values for wind shear exponent, turbulence intensity, current speed and current direction are assumed and used in the modelling process, which are: 0.14, 0.07, 0.25 m/s and 60 deg. However, it is worth noting that more realistic modelling of current, like different current speed and current direction corresponds to different wind speed and wind direction can be handled by the model. Also note that the sea depth at this site is assumed to be 200 m for this case study to match the turbine surrogate setting, while the real sea depth of 85.5 m is not considered here, as it would have required to redesign the mooring lines.

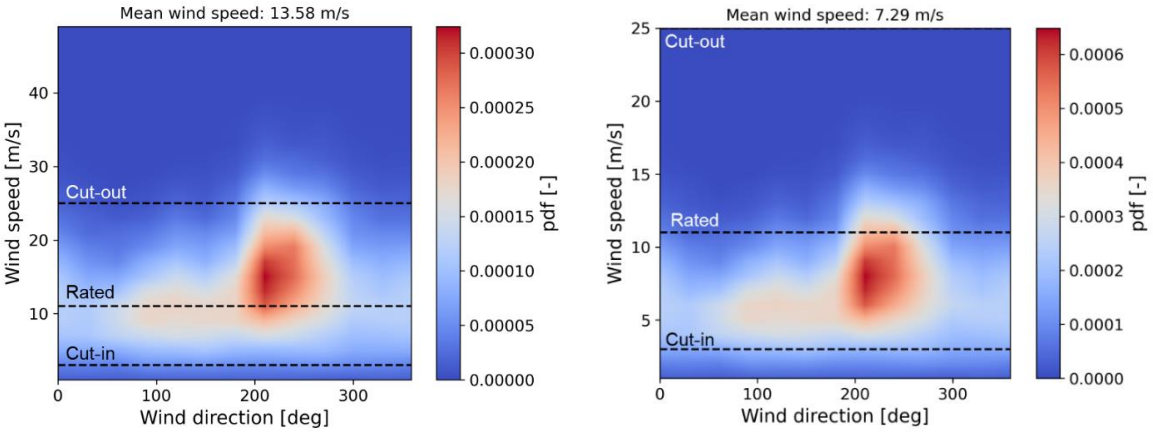


**Figure 7.** Joint distribution of wind speed and wind direction for the original (left) and reduced (right) wind conditions.

*4.2. FOWF with 11 turbines*

Considering a FOWF composed of 11 FOWTs and assuming its original layout is a staggered grid-like layout with 5 rotor diameters spacing between rows and columns, we can then optimize its layout to maximize the expected AEP.

In this study, the circular wind farm boundary is assumed to have its centre coinciding with the central turbine location and with the radius to just cover all the turbines. And the minimal spacing is set as 4 rotor diameters, i.e., $d_{min} = 960$ m. Under this setting, layout optimization is carried out for both the original and the reduced wind conditions, using RS with 10000 steps. The results are shown in Figure 8 and 9. Note that the position of the central turbine (#5) in the optimized layouts has been slightly changed, although this is not obvious in the figures.

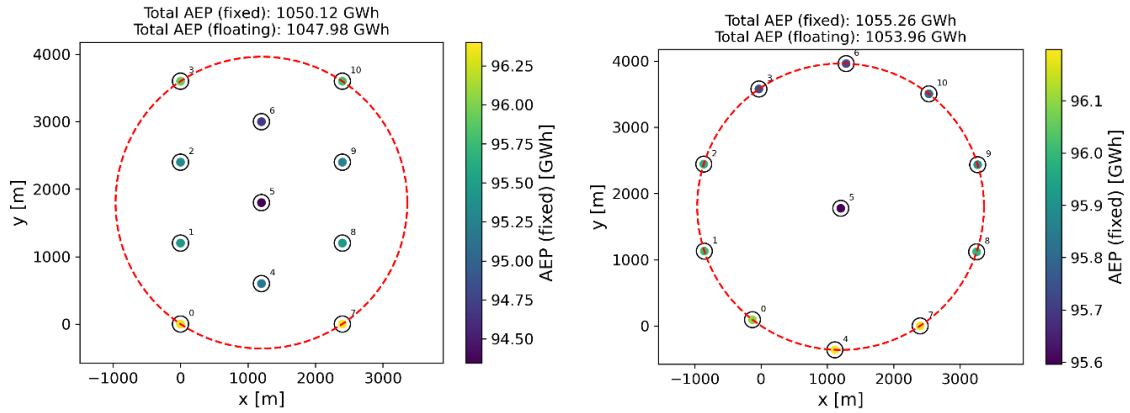


**Figure 8.** Original (left) and optimized (right) layouts of the wind farm with 11 turbines under the original wind condition, with red dashed line representing the wind farm boundary.

Note that in view of the computational cost difference, the optimization is done with the fixed version of model, i.e., treating FOWTs as bottom-fixed, and then re-evaluated using the floating version of model. Thus, there are two sets of total AEP values shown in Figures 8 and 9. As shown in both wind conditions, the optimized layout yields decent AEP increases, no matter if evaluated as fixed or floating.

To further check the validity of the results, the evolution histories of the optimization runs are also re-evaluated using the floating version of model. Note that the evolution history of a given RS optimization run is composed of a list of improved layouts, i.e., out of the total 10000 steps, all the steps that obtain a layout better than the current best layout are stored in the history. Therefore, this history shows how the layout has been improved in the optimization process and demonstrates the efficiency of

the optimization process. The original (solid blue) and the re-evaluated (dashed orange) evolution histories are shown in Figure 10 for both the original wind condition and the reduced wind condition.

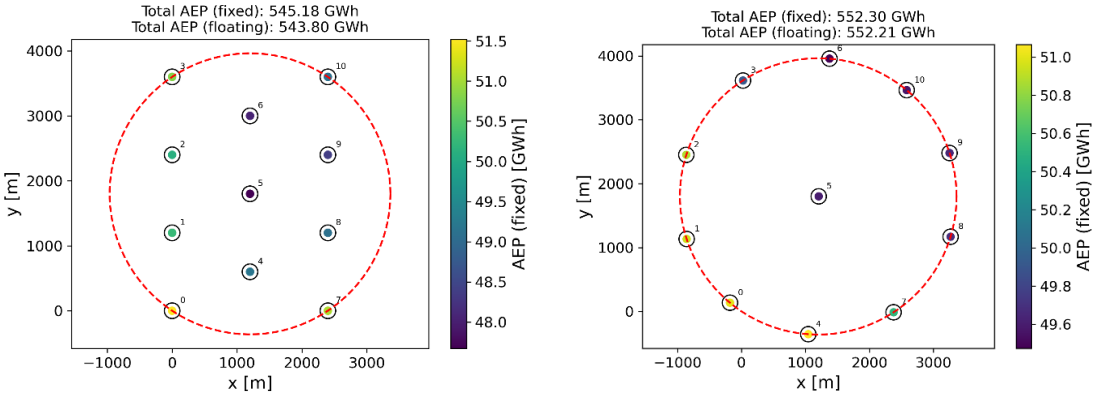


**Figure 9.** Original (left) and optimized (right) layouts of the wind farm with 11 turbines under the reduced wind condition, with red dashed line representing the wind farm boundary.

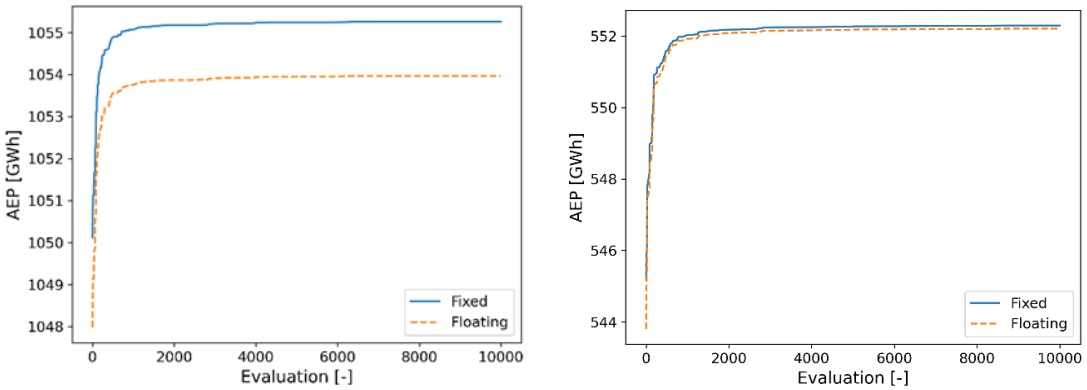


**Figure 10.** Original (fixed) and re-evaluated (floating) evolution histories of the optimization processes for both the original (left) and the reduced (right) wind conditions.

As we can see from Figure 10, although there are absolute differences between the original and the re-evaluated histories, they follow almost the same trend in both wind conditions. This means the method to optimize the layout with the fixed version of model and then re-evaluate with the floating version of model can be a reasonable choice in the current setting of the layout optimization problem.

### *4.3. FOWF with 23 turbines*

For a FOWF with 23 turbines, similar results are obtained as shown in Figure 11 and 12.

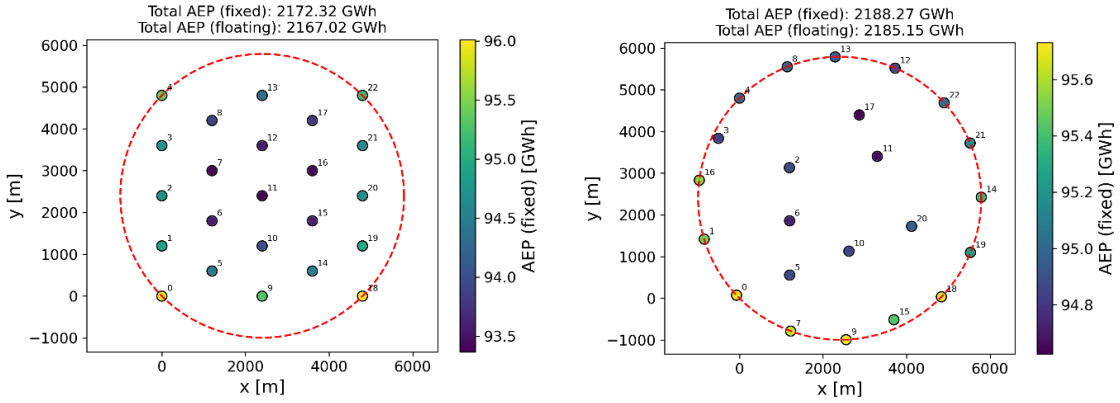


**Figure 11.** Original (left) and optimized (right) layouts of the wind farm with 23 turbines under the original wind condition, with red dashed line representing the wind farm boundary.

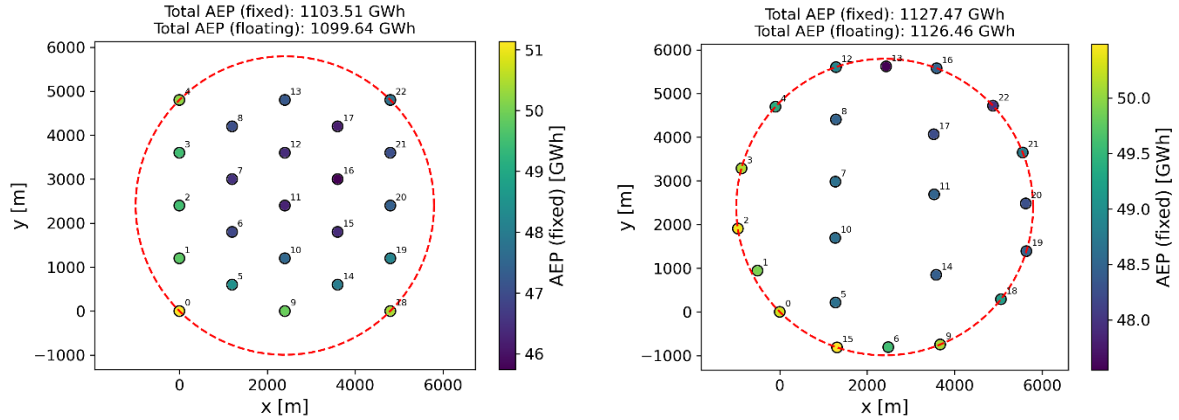


**Figure 12.** Original (left) and optimized (right) layouts of the wind farm with 23 turbines under the reduced wind condition, with red dashed line representing the wind farm boundary.

Note that in this case, similar setting with regards to the original layout, circular wind farm boundary and same minimal spacing (of 4 rotor diameters) are assumed. And the layout optimization is also done for both the original and the reduced wind conditions, using RS with 10000 steps. And we can also observe similar AEP improvements under both wind conditions from these figures.

### *4.4. Summary of results*

To gain a systematic understanding of the results, we tabulate the results into Table 3.

**Table 3.** Summary of optimization results for the two FOWFs (with 11 and 23 FOWTs) under original and reduced wind conditions

| Number of FOWTs | Modelling version | Original wind condition | | | Reduced wind condition | | |
|---|---|---|---|---|---|---|---|
| | | AEP [GWh] | | Imp. [%] | AEP [GWh] | | Imp. [%] |
| | | Original | Optimized | | Original | Optimized | |
| 11 | Fixed | 1050.12 | 1055.26 | 0.49 | 545.18 | 552.30 | 1.31 |
| | Floating | 1047.98 | 1053.96 | 0.57 | 543.80 | 552.21 | 1.55 |
| 23 | Fixed | 2172.32 | 2188.27 | 0.73 | 1103.51 | 1127.47 | 2.17 |
| | Floating | 2167.02 | 2185.15 | 0.84 | 1099.64 | 1126.46 | 2.44 |

By comparing different numbers in this table, we can see that: (1) the fixed version of model reports a higher AEP comparing to the floating version, with the absolute differences more profound for the larger FOWFs and/or higher wind conditions, which may be caused by the fact that each FOWT will produce less power under the same inflow wind speed comparing to its fixed counterpart due to the tilted rotor, while the resulted deflection of wakes behind FOWTs has a less overall impact on the power output of the wind farm; (2) similar relative AEP improvements are reported by the two versions of models, while in general the increase percentage obtained by the floating version of model tends to be slightly higher; (3) layout optimization can yield higher percentages of AEP improvements for larger wind farms and/or lower wind conditions, which can be explained by the relatively higher wake losses, thus higher potential to improve, under these scenarios.

## 5. Conclusions

In this study, we demonstrated how to consider the steady state movements of the FOWTs in the modelling of flow and power production of FOWFs, by using a recently proposed steady state movement and flow model for FOWFs. This model couples an ANN based turbine surrogate model trained on `HAWC2` simulations with a static wind farm simulator `PyWake` to simulate the steady state movements of FOWTs and the steady state flow inside the FOWF under different met-ocean conditions. Based on

this model, the layout optimization problem of FOWFs is formulated to maximize AEP, while satisfying constraints on wind farm boundary and minimal spacing. The problem is then solved with the Random Search algorithm. The used FOWT is the IEA 15MW reference wind turbine with the WindCrete spar floater. Case study at the Havbredey FOWF project site in Scotland was then conducted, which demonstrated the potential of layout optimization for floating wind. It was also found that this potential is higher for larger FOWFs and/or lower wind condition sites. Also, we have shown that for the current problem setting, we can speed up the optimization process by treating FOWTs as bottom-fixed when running optimizations and then re-evaluating the found layouts by treating them as floating turbines.

Future studies will extend the design optimization scope, by including mooring line lengths, anchor positions, and other factors in the list of design variables. Also more sites with different site conditions and FOWFs with different number and types of FOWTs will be studied to examine the validity of the findings obtained in this study.

**Acknowledgements**
This work has been supported by the IDEA project funded by the Danish Energy Technology Development and Demonstration Program (EUDP) under project number 134-21029. Discussions with many colleagues in the IEA Wind Task 49 are also much appreciated.

**References**
[1] Equinor, *Hywind Scotland*, accessed at: https://www.equinor.com/energy/hywind-scotland
[2] Díaz, H., Serna, J., Nieto, J., & Guedes Soares, C. (2022). Market needs, opportunities and barriers for the floating wind industry. *Journal of Marine Science and Engineering*, *10*(7), 934.
[3] Hou, P., Zhu, J., Ma, K., Yang, G., Hu, W., & Chen, Z. (2019). A review of offshore wind farm layout optimization and electrical system design methods. *Journal of Modern Power Systems and Clean Energy*, *7*(5), 975-986.
[4] Liang, Z., & Liu, H. (2022). Layout optimization of a modular floating wind farm based on the full-field wake model. *Energies*, *15*(3), 809.
[5] Riva, R., Pedersen, M.M., Pirrung, G., Bredmose, H., & Feng, J. (2024). Incorporation of floater rotation and displacement in a static wind farm simulator. *Journal of Physics: Conference Series*, *2767*(6), 062019.
[6] Pedersen, M.M., van der Laan, P., Friis-Møller, M. & et al. (2023) *PyWake 2.5.0: An open-source wind farm simulation tool*, Technical University of Denmark. Software available at: https://topfarm.pages.windenergy.dtu.dk/PyWake/
[7] Feng, J., & Shen, W. Z. (2015). Solving the wind farm layout optimization problem using random search algorithm. *Renewable Energy*, *78*, 182-192.
[8] Gaertner, E., Rinker, J., Sethuraman, & et al. (2020). *Definition of the IEA 15-Megawatt Offshore Reference Wind Turbine*. National Renewable Energy Laboratory (NREL).
[9] Mahfouz, M., Salari, M., Hernández, S., Vigara, F., Molins, C., Trubat, P., Bredmose, H. & Pegalajar-Jurado, A. (2020) *COREWIND D1.3: Public design and FAST models of the two 15MW floater-turbine concepts*. Technical report, University of Stuttgart.
[10] Santos, P. (2023). *Havbredey Preliminary Metocean Study*. DHI Technical Report (Project No 11826846).
[11] Larsen, T.J. & Hansen. A.M. (2021) *How 2 HAWC2, the user's manual*. Technical report, Technical University of Denmark.
[12] Abadi, M., Agarwal, A., Barham, P., & et al. (2015). *TensorFlow: Large-scale machine learning on heterogeneous systems*. Software available from tensorflow.org.
[13] Feng, J., Shen, W. Z., & Xu, C. (2016). Multi-objective random search algorithm for simultaneously optimizing wind farm layout and number of turbines. *Journal of Physics: Conference Series*, *753*(3), 032011.
[14] Brogna, R., Feng, J., Sørensen, J. N., Shen, W. Z., & Porté-Agel, F. (2020). A new wake model and comparison of eight algorithms for layout optimization of wind farms in complex terrain. *Applied Energy*, *259*, 114189.